Thermal Expansion Behavior in TcO$_2$. Towards breaking the Tc-Tc bond.

Emily Reynolds[†], Zhaoming Zhang[‡], Maxim Avdeev[‡], Gordon J. Thorogood[‡], Frederic Poineau[§], Kenneth R Czerwinski[§], Justin A. Kimpton[¶] and Brendan J. Kennedy[‡*]

†Inorganic Chemistry Laboratory, University of Oxford, South Parks Road, OX1 3QR UK
‡Australian Nuclear Science and Technology Organisation, Lucas Heights, NSW 2234 Australia,
§University of Nevada Las Vegas, Department of Chemistry and Biochemistry, 4505 Maryland Parkway, 89154 Las Vegas, NV USA
¶Australian Synchrotron, 800 Blackburn Rd, Clayton, Victoria 3168, Australia.
‡School of Chemistry, The University of Sydney, Sydney, NSW 2006 Australia

ABSTRACT: The structure of TcO$_2$ between 25 and 1000 °C has been determined *in-situ* using powder diffraction methods and is found to remain monoclinic in space group $P2_1/c$. The thermal expansion in TcO$_2$ is highly anisotropic with negative thermal expansion of the *b*-axis observed above 700 °C. This is the result of an anomalous expansion along the *a*-axis that is a consequence of weakening of the Tc-Tc bonds.

Introduction

Technetium is the lightest element that does not have a stable isotope. The most abundant isotope is ^{99}Tc, which is a soft β emitter (292 keV) with half-life of 2.11 x 10^5 years, that forms as a product of the fission of uranium in a mass yield of 6.1%. The efficient and safe management of nuclear waste is significantly impacted by the presence of ^{99}Tc, in terms of both the amount of radiation produced and the mobility of this in the environment. Paradoxically ^{99m}Tc, with a half-life of 6 hours, is the most commonly used medical radioisotope and this is produced by the neutron irradiation of Mo to form ^{99}Mo in uranium fission reactors. Currently there is no agreed optimal method to manage ^{99}Tc, reflecting the paucity of knowledge regarding the stability of the oxide phases that will be involved in its long term storage [1] and more fundamental studies of technetium oxides are essential [2].

The room temperature structure of technetium dioxide TcO$_2$, the simplest of the technetium oxides, has been studied using X-ray powder diffraction (XRD) [3], neutron powder diffraction (NPD) [4] and X-ray absorption spectroscopy (XAS) [5]. Muller and co-workers [6] described TcO$_2$ as having a distorted rutile structure and, following Magneli and Anderson [7], proposed that this was isostructural with MoO$_2$. This proposal was confirmed in the recent neutron diffraction study of Rodriguez *et al.* [4] who successfully refined the structure in space group $P2_1/c$. The tetragonal rutile structure is based on edge-sharing chains of MO$_6$ that run along the [001] direction with the metal atoms equidistant in the chain, see Figure 1. In the monoclinic MoO$_2$ structure strong M-M interactions between the unpaired 4d valence electrons cause the structure to distort, results in the formation of Mo –Mo pairs and each Mo –Mo

pair tilts away from *a* to create alternating short (2.508 Å) and long (3.114 Å) Mo –Mo separations along the *a* axis in such a way that the cations along the edge-sharing chains move closer and further away [8]. In space group $P2_1/c$ the chains of edge sharing octahedra are along [100].
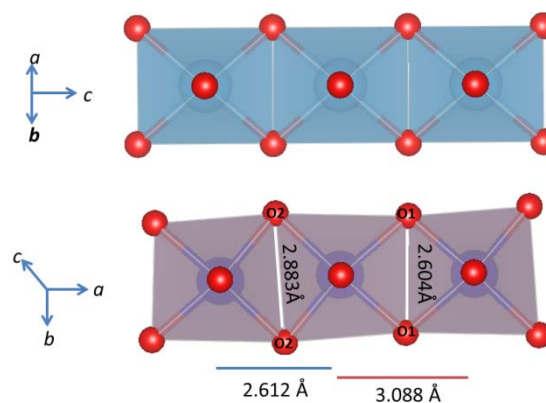
Figure 1. Comparison of the TiO$_2$ rutile and TcO$_2$ structures. The changes in the Tc-Tc distances along the *a*-axis are highlighted by different colours for different Tc-Tc lengths, and the effect of Tc-Tc dimerization on the separation of the anions across the shared edge is illustrated. The red spheres represent the anion oxygens and the cations are at the centre of the polyhedra.

1

There is considerable interest in low dimensional oxides containing transition metals due to their unique electronic and magnetic properties. Systems containing early 4*d* and 5*d* transition metals, especially Mo, Ru, W and Re, can potentially exhibit direct metal to metal (*M-M*) bonding between the transition metal cations, as evident in MoO_2 and other oxides containing one-dimensional infinite chains such as $Ln_2Mo_5O_{12}$ (*Ln* = lanthanoid) [9] [10] or $Y_5Re_2O_{12}$ [11] and in lower dimensional oxides such as Li_2RuO_3 [12]. Whilst *M-M* bonding in molecular compounds has been extensively studied, there is a paucity of reports of oxides with *M-M* bonds. Thermally induced breaking of *M-M* bonds is rare although it is observed in VO_2 which, in its low temperature insulating phase, is isostructural with TcO_2. Above 340 K VO_2 adopts the regular rutile structure and is metallic [13, 14]. Understanding the metal insulator transition of VO_2 remains problematic despite the vast number of studies of this oxide [15, 16]. It is generally accepted that the metal-insulator transition in VO_2 is a consequence of breaking of the *M-M* bonds formed between VO_6 polyhedra [17].

There have been a number of studies of the environmental stability of TcO_2, both in terms of its dissolution in water and its precipitation from solutions of technetium[18]. In oxygenated environments, Tc(VII) is soluble and mobile as the pertechnetate ion (TcO_4^-), but under reducing conditions, it precipitates as Tc(IV) species. Iron(II)-containing minerals are able to reduce Tc(VII) to Tc(IV) abiotically [19]. The high temperature behaviour of solid TcO_2, to our knowledge, has never been reported. The present work describes the investigation of the high temperature behaviour of TcO_2 *in-situ* using SXRD and NPD and we show a remarkable weakening of the Tc-Tc interactions upon heating, and compare the observed structural changes to those seen in other rutile type oxides.

Experimental

Caution! ^{99}Tc is a β- emitter (E_{max} = 0.29 MeV). All manipulations were performed in a laboratory designed for radioactivity using efficient HEPA-filtered fume hoods, and following locally approved radiochemistry handling and monitoring procedures. Laboratory coats, disposable gloves, and protective eyewear were worn at all times. Samples were transported in approved containers.

Synchrotron X-ray powder diffraction (SXRD) data were collected over the angular range 5 < 2θ < 85°, using X-rays of wavelength 0.72800 Å, calibrated using a NIST SRM 660b LaB_6 standard, on the powder diffractometer at beamline BL-10 of the Australian Synchrotron[20]. The sample (~ 3 mg) was housed in a 0.3-mm-diameter quartz capillary, which were rotated during the measurements. The capillary was flame sealed for protection against the spread of radiological material. The data were obtained using a bank of 16 Mythen detectors, each of which covers 5 degrees of data. Diffraction data were collected for 5 min at each of the two detector positions, to avoid gaps in the data from the individual modules. Neutron powder diffraction experiments were performed on a 2g sample sealed in 6 mm diameter vanadium can at the high-resolution powder diffractometer Echidna[21] at ANSTO's OPAL facility at Lucas Heights. The SXRD and NPD data were refined by the Rietveld method using the GSAS refinement program [22]. A pseudo-Voigt function was chosen to generate the line shape of the diffraction peaks. No regions were excluded in the refinements against the SXRD data. The following parameters were refined in the final analysis: scale factor, zero-point error, background (12 (neutron) or 24

(SXRD) term shifted Chebyschev) coefficients, lattice parameters, positional coordinates and isotropic atomic displacement.

X-ray absorption near edge structure (XANES) spectra were collected from TcO_2 and $SrTcO_3$ standard at the Tc K-edge on beamline BL-12 [23] at the Australian Synchrotron in transmission mode using argon-filled ionisation chambers [24]. 2 mg of Tc-containing powder sample was first mixed with an appropriate amount of BN, and the mixture was then loaded into a 3.5 mm diameter hole at the centre of a 1 mm thick Al plate. The samples were sealed using two Kapton tapes on both sides of the Al plate. The energy calibration was carried out using the Mo K-edge at 20000 eV. The software package Athena was used for background subtraction and normalisation [25].

Results and Discussion

Room temperature structure

The synthesis of TcO_2 was achieved via the decomposition of $(NH_4)TcO_4$ under an Ar atmosphere at 750 °C. The synchrotron X-ray diffraction (SXRD) pattern of the sample was well fitted using the monoclinic $P2_1/c$ model described by Rodriguez *et al.*,[4] and there was no evidence for any crystalline impurities. Subsequently the structure was refined against a combined SXRD and Neutron Powder Diffraction (NPD) data set and as evident from Figure 2 and Table 1 this resulted in acceptable fits to both data sets. The SXRD data provide more precise information on the lattice parameters and cation position, whereas the NPD data give much more precise information on the oxygen positions. As described previously TcO_2 has a distorted rutile-type structure with alternating short and long Tc-Tc bond distances of 2.612(1) and 3.088 (1) Å respectively. There are two crystallographic distinct anions and the average Tc-O1 and Tc-O2 distances, 2.006(3) Å and 1.960(3) Å, are essentially identical. These structural features are in good agreement with the literature [4].
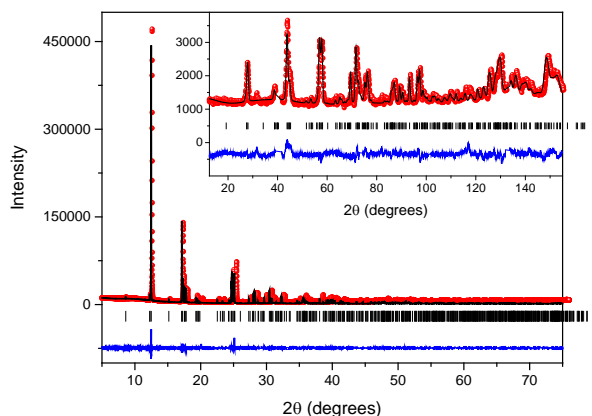

Figure 2. Rietveld refinements of SXRD and (inset) NPD data of TcO_2 at room temperature. The lower line is the difference between the data (symbols) and the calculated profile (solid line). The vertical markers show the positions of the Bragg reflections allowed by space group $P2_1/c$. The gaps in the neutron profile are excluded regions containing reflections form the Nb heating elements of the furnace.

X-ray absorption near-edge structure (XANES)

The normalised Tc K-edge XANES spectrum of TcO$_2$ at room temperature is shown in Figure 3. The spectrum of the perovskite SrTcO$_3$, in which Tc exists in a tetravalent state in an octahedral environment, is also shown. Whilst the energy of the absorption edge of the two oxides is similar and consistent with the Tc^{4+} state, there are significant differences in the lineshape of the two spectra. These differences reflect the greater distortion in TcO$_2$ as a result of the Tc-Tc pairing.
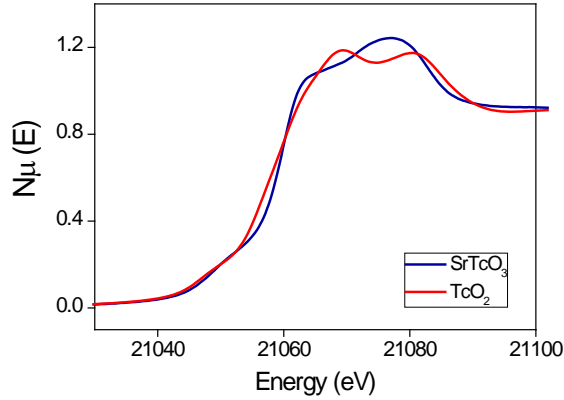

Figure 3. Normalised Tc K-edge XANES spectra of TcO$_2$, and SrTcO$_3$. The similarity in the edge position demonstrates the presence of Tc^{4+} in both oxides.

High temperature synchrotron X-ray and neutron powder diffraction

Muller *et al*. reported that TcO$_2$ was stable up to 1100 °C, although they did not investigate the temperature dependence of the structure [6]. The high temperature behaviour of the structure of TcO$_2$ was investigated using SXRD and NPD. The temperature dependence of the unit cell parameters obtained by Rietveld refinement against SXRD data are shown in Figure 4. The thermal expansion of TcO$_2$ is anisotropic. Positive thermal expansion of the *c* lattice parameter was observed over the whole temperature range studied (25-1000 °C). However, whilst approximately linear positive thermal expansion was observed for the *a* and *b* lattice parameters below 600 °C, at temperature above this the rate of expansion of the *b* lattice parameter changed with temperature exhibiting a maximum near 700 °C and negative thermal expansion at temperatures above this. The rate of thermal expansion along the *a*-axis is observed to increase more rapidly above 700 °C. The monoclinic angle mirrors the thermal expansion along the *b*-axis, decreasing to a minimum value near 700 °C, above which it begins to increase. Despite this unusual behaviour there is no evidence for any structural transition, and the *P*2$_1$/*c* model fits the data up to 1000 °C. Indeed the unit cell volume showed typical positive thermal expansion. Fitting this to a quadratic function showed there was small deviation from this at the highest temperatures, although no additional reflections were evident in the diffraction pattern suggesting little, if any, decomposition of the sample had occurred.

Table 1 Structural parameters of TcO$_2$ at room temperature and at 900 °C refined against combined SXRD and NPD data sets.

Temp (°C)	25	900
a (Å)	5.6918(2)	5.7562(2)
b (Å)	4.7621(2)	4.7752(2)
c (Å)	5.5231(2)	5.5605(2)
β (°)	121.5457(4)	121.4875(2)
Vol (Å^3)	127.58(1)	130.336(8)
Tc	4e (*x,y,z*)	
x	0.2631(1)	0.2613(1)
y	1.0048(4)	1.0067(3)
z	-0.0155(1)	-0.0126(1)
U$_{iso}$ x100 (Å^2)	0.51(1)	1.34(1)
O1	4e (*x,y,z*)	
x	0.1043(5)	0.0946(6)
y	0.1897(5)	0.2005(7)
z	0.1953(5)	0.1945(6)
U$_{iso}$ x100 (Å^2)	1.13(4)	2.35(7)
O2	4e (*x,y,z*)	
x	0.3906(5)	0.3864(6)
y	0.7096(5)	0.7039(6)
z	0.2731(4)	0.2767(6)
U$_{iso}$ x100 (Å^2)	1.01(4)	2.52(7)
R$_p$ (NPD)	0.0376	0.0342
R$_p$ (SXRD)	0.0477	0.0372
R$_p$ (Total)	0.0472	0.0343
R$_{wp}$ (Total)	0.0582	0.0501
Tc-O1 (Å)	2.012(2)	2.063(3)
Tc-O1 (Å)	2.011(3)	2.008(3)
Tc-O1 (Å)	1.994(3)	1.974(3)
Tc-O2 (Å)	1.958(3)	1.996(3)
Tc-O2 (Å)	1.967(3)	1.986(3)
Tc-O2 (Å)	1.954(2)	1.946(3)
Tc-O$_{(avg)}$ (Å)	1.983	2.005
Δd x 10^4	5.78	12.9
BVS	4.02	3.90
Tc-Tc (Å)	2.612(1)	2.679(1)
Tc-Tc (Å)	3.088(1)	3.084(1)

Following Rogers *et al*.[26] the *c/a* ratio for the rutile pseudo-cell of TcO$_2$ was estimated as $c/a = a/(b + c \sin\beta)$. The *c/a* ratio for the monoclinic MoO$_2$ type oxides is systematically smaller than that of the tetragonal rutiles and Rogers and co-workers [26] concluded that this is indicative of *M-M* interactions with the length of the shorter *M - M* distance reflecting the strength of the bond. Bolzan *et al*. [27] postulated that, even in the absence of the dimerization observed in the MoO$_2$ type oxides, metallic bonding in rutiles results in a contraction in *c* and consequently a small *c/a* ratio. As evident from Figure 4 the *c/a* ratio in TcO$_2$ initially decreases upon heating and then increases. Remarkably there are relatively few crystallograph-

ic studies of the thermal expansion of rutile type dioxides. It appears that for TiO_2 itself both a and c increase with increasing temperature, such that the c/a ratio shows a small approximately linear increase [28]. A similar situation occurs for the high temperature tetragonal phase of VO_2. Conversely for MnO_2 the c/a ratio decreases, approximately linearly, upon heating [29]. Caution must be exercised in extrapolating from these observations, since the literature studies typically cover limited temperature ranges and were conducted at relatively coarse temperature intervals. Nevertheless it is tempting to postulate that the non-linear change in the c/a ratio in TcO_2 is significant and is indicative of a weakening of the Tc-Tc interactions above ~ 700 °C. Evidence to support this postulate comes from the temperature dependence of the Tc-Tc distances shown below.

As illustrated in Figure 5 both the short and long Tc-Tc distances in TcO_2 initially increase upon heating, although the rate of increase of the shorter Tc-Tc distance is clearly greater. That both distances initially increase is not surprising given the increase in the unit cell volume, illustrated in Figure 4. Around ~ 600 °C the rate of increase of the shorter Tc-Tc distance increases, such that at 1000 °C this distance is approximately 3% larger than the value estimated from a linear extrapolation of the expansion between 25 and 600 °C. The longer Tc-Tc distance reaches a maximum value near ~ 600 °C and then this begins to decrease. In the ideal tetragonal rutile structure these two distances would be equal, however a transition to such an arrangement appears remote. The temperature dependence of the short Tc-Tc distance mimics that of the a lattice parameter, reflecting the fact that the edge-sharing TcO_6 chains run along [100] in the monoclinic cell. Based on the changes in both the c/a ratio and the Tc-Tc distances it seems reasonable to conclude that the strong Tc-Tc bonding weakens as the temperature increases.
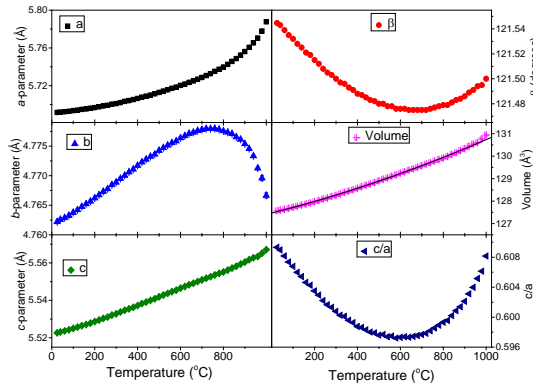

Figure 4. Temperature dependence of the lattice parameters, unit cell volume and rutile c/a ratio extracted from Rietveld refinements of SXRD data of TcO_2.

The onset of the weakening of the Tc-Tc bond coincides with the other structural changes, and is presumably the cause of these. In general when M-M bonded dimers form the metal ion shifts from the octahedron centre in the direction of the corresponding octahedral edge, and the octahedra experiences a large distortion. This is most evident in the O-Tc-O bond angles in TcO_2. The formation of the Tc-Tc bond results in repulsion of the two bridging oxygen anions away from each other and at all temperatures the O2-O2 distance across the

shorter shared edge is significantly longer than the O1-O1 distance across the longer shared edge, the values at room temperature being 2.883 vs 2.604 Å. This displacement of the O2 anions allows direct overlap between the Tc t_{2g} orbitals. The displacement of the anions is also evident from the bond-angles with the Tc-O1-Tc angle being noticeably larger than the Tc-O2-Tc angle, 94.1(3) vs 81.7(4)°. Heating the sample to 900 °C reduced the anisotropy in these with the O2-O2 distance decreasing to 2.813 Å and the O1-O1 distance increasing to 2.716 Å and bond angles changing to 92.4(4) and 83.5(4) ° for Tc-O1-Tc and Tc-O2-Tc respectively.
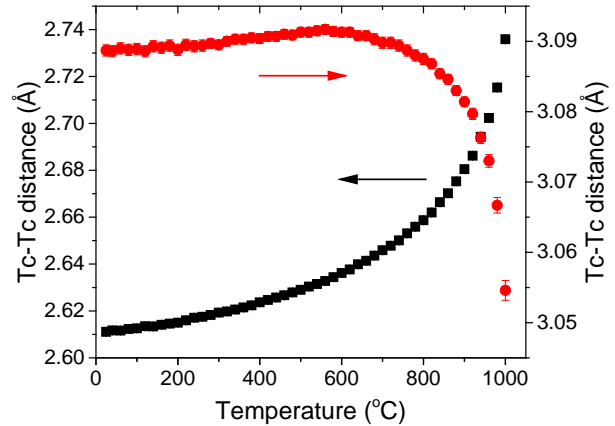

Figure 5. Temperature dependence of the Tc-Tc distances in TcO_2 established by Rietveld refinements against SXRD data. Where not apparent the esds are smaller than the symbols.

The distortion of the TcO_6 octahedra can be quantified using the quantity $\Delta d = \frac{1}{6}\sum(\frac{d_i - d_m}{d_m})^2$ where d_m is the average Tc-O distance and d_i the individual Tc-O distance. The distortion of the TcO_6 octahedra at room temperature, $\Delta d = 5.8 \times 10^{-4}$, is greater than that observed in TiO_2 (2.1 x 10^{-4}) but is less than that observed in the monoclinic oxides WO_2 (15.7 x 10^{-4}) and MoO_2 (21.5 x 10^{-4}). VO_2 has a still greater distortion, 112 x 10^{-4}. Rogers et al. [26] postulated that as the M-M distance shortens the distortion of the MO_6 octahedra increases, this is not the case since the Tc-Tc distance is similar to the V-V distance in VO_2 but the distortion of the MO_6 octahedra are very different. There is a systematic increase in Δd of TcO_2 upon heating evident from analysis of the NPD data. Due to the limited number of temperatures studied by NPD (8) compared to SXRD (48) and the lower signal to noise in the NPD data, it is not feasible to comment further on this.

Considering now the anisotropy of the thermal expansion, recall that anisotropic thermal expansion is not unusual in metal oxides and can arise from cooperative displacements of semi-rigid polyhedra, often described by rigid unit mode (RUM) analysis. Negative thermal expansion (NTE) can result in the extreme RUMs. In the present case the distortion of the TcO_6 octahedron suggests such an approach is inappropriate. The linear thermal expansion coefficients (TEC) in TcO_2 between 25 and 600 °C, defined as $\alpha_l = \frac{(l_{600} - l_{25})}{l_{25}*\Delta T}$ where l is the appropriate unit cell parameter (a, b or c) and ΔT the change in temperature, are approximately equal, 8.74, 5.2 and 7.5 x 10^{-6} K^{-1} for a, b and c respectively. Since the unit cell volume shows conventional thermal expansion (the average

linear TEC $\bar{\alpha}$ between 25 and 1000 °C, calculated in a similar manner using the cube root of the volume, is 11.3 x 10^{-6} K^{-1}) the expansion in a that occurs above 600 °C in response to the weakening of the Tc-Tc bond needs to be compensated by contraction elsewhere and this drives the unusual thermal response of the lattice parameter b and the monoclinic β angle. The TEC along the b-axis around 1000 °C is -24.9 x10^{-6} K^{-1}. This compares to the TEC in NTE materials such as -7.2x$10^{-6}K^{-1}$ for ZrW_2O_8 [30] or -33×10^{-6} K^{-1} for $Cd(CN)_2$ [31].

Finally we address the question of why TcO_2 is so different to VO_2. Comparing the short M-M distance for the isostructural series VO_2, MoO_2 and TcO_2 (2.619, 2.508 and 2.612 Å respectively) it appears that the Tc-Tc and V-V bond orders are one whereas the Mo-Mo bond order is two [4, 26]. This can be explained using the molecular orbital (MO) approach of Goodenough where for the d^1 dimers in VO_2 the electrons form a σ type M-M bond [32]. For the d^2 dimers of MoO_2 the additional electrons occupy a M-M π type orbital. Due to distortion of the octahedra the degeneracy of the t_{2g} orbitals is lifted and for the d^3 dimers in TcO_2 the next level occupied is a M-M π^* type orbital which weakens the M-M bonding. The formation of a single σ type M-M bond has been validated by DFT calculations [4], that reveals broadening of the bands as a consequence of the diffuse nature of the 4d orbitals. Similar broadening is expected to occur for TcO_2. Since the bond order in TcO_2 is comparable to that of VO_2 (with a metal-insulator transition temperature, T_{MI} ~340K [32]) and NbO_2 (which has a subtly different structure and T_{MI}~1070 K [33]), it is not unreasonable that the dimerization of the Tc ions may be broken down by heating to modest temperatures. Such a transition is expected to be a metal-metal transition, rather than the insulator-metal transition observed in VO_2 and NbO_2. More sophisticated analysis including cluster [34] and DFT [35] calculations, augmented by high resolution X-ray photoemission spectroscopy [35], of MoO_2 have demonstrated that splitting of the t_{2g} orbitals occurs as described by Goodenough[32]. Whilst the Goodenough model provides a clear explanation for the relative bond M-M strengths in these types of oxides, it does not explain the thermally induced weakening of the Tc-Tc bond, since an electron thermally excited from the M-M π^* type orbital is likely to occupy a δ type MO, see Figure 6.
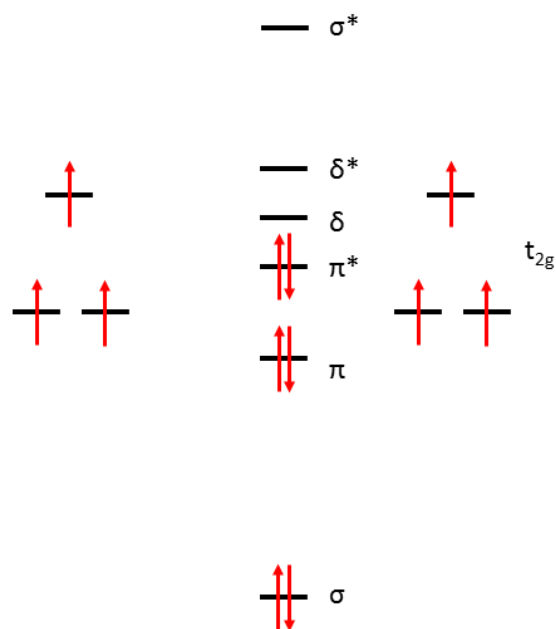

Figure 6. Molecular orbital ordering diagram for the d-electrons involved in forming the metal-metal bond in TcO_2.

Conclusions

It is demonstrated that TcO_2 is stable to 1000 °C, and that the structure remains monoclinic in space group $P2_1/c$ to this temperature. The thermal expansion in TcO_2 is highly anisotropic with negative thermal expansion of the lattice parameter b observed above 700 °C. This is a consequence of an anomalous expansion along the a-axis that is a consequence of weakening of the Tc-Tc bonds. Whereas in the isostructural d^1 oxide VO_2 the V-V bond is broken on heating, resulting in a transition to the regular rutile structure, the tetragonal rutile structure is not formed in TcO_2 up to 1000 °C. It is possible that the rutile structure will form in TcO_2 at higher temperatures, however experimentally accessing this is problematic due to the radioactive nature of Tc. Irrespective of this, that the Tc-Tc bond gradually weakens upon heating is unusual and is apparently not duplicated in VO_2. Whilst the MO described by Goodenough [32] can be used to explain the effect of increasing the d-orbital occupancy on the formation and relative strength of the metal-metal bonds in MoO_2 type oxides and explains the relative stability of the regular versus distorted rutile structure in TiO_2, VO_2 and MoO_2 it does not provide a reason for the thermally induced weakening of the Tc-Tc bond observed in this work. Since TcO_2 with a regular rutile structure is expected to be metallic, establishing the importance of metallic conductivity on the stability of the M-M bonds in rutile type oxides is clearly worthy of investigation.

AUTHOR INFORMATION

Corresponding Author

* Brendan.Kennedy@Sydney.edu.au

Author Contributions

The manuscript was written through contributions of all authors. All authors have given approval to the final version of the manuscript.

REFERENCES

(1) Darab, J. G.; Smith, P. A. Chemistry Of Technetium And Rhenium Species During Low-Level Radioactive Waste Vitrification. *Chem. Mater.,* **1996,** 8, 1004-1021.

(2) Weaver, J.; Soderquist, C. Z.; Washton, N. M.; Lipton, A. S.; Gassman, P. L.; Lukens, W. W.; Kruger, A. A.; Wall, N. A.; McCloy, J. S. Chemical Trends in Solid Alkali Pertechnetates. *Inorg. Chem.,* **2017,** 56, 2533-2544.

(3) Silva, G. W. C.; Poineau, F.; Ma, L. Z.; Czerwinski, K. R. Application of Electron Microscopy in the Observation of Technetium and Technetium Dioxide Nanostructures. *Inorg. Chem. ,* **2008,** 47, 11738-11744.

(4) Rodriguez, E. E.; Poineau, F.; Llobet, A.; Sattelberger, A. P.; Bhattacharjee, J.; Waghmare, U. V.; Hartmann, T.; Cheetham, A. K. Structural studies of TcO_2 by neutron powder diffraction and first-principles calculations. *J. Am. Chem. Soc.,* **2007,** 129, 10244-10248.

(5) Almahamid, I.; Bryan, J. C.; Bucher, J. J.; Burrell, A. K.; Edelstein, N. M.; Hudson, E. A.; Kaltsoyannis, N.; Lukens, W. W.; Shuh, D. K.; Nitsche, H.; Reich, T. Electronic And Structural Investigations Of Technetium Compounds By X-Ray-Absorption Spectroscopy. *Inorg. Chem.,* **1995,** 34, 193-198.

(6) Muller, O.; White, W. B.; Roy, R. Crystal Chemistry Of Some Technetium-Containing Oxides. *J. Inorg. Nucl. Chem.,* **1964,** 26, 2075-2086.

(7) Magneli, A.; Andersson, G. On The MoO_2 Structure Type. *Acta Chem. Scand.,* **1955,** 9, 1378-1381.

(8) Bolzan, A. A.; Kennedy, B. J.; Howard, C. J. Neutron Powder Diffraction Study Of Molybdenum And Tungsten Dioxides. *Aust. J. Chem.,* **1995,** 48, 1473-1477.

(9) Colabello, D. M.; Camino, F. E.; Huq, A.; Hybertsen, M.; Khalifah, P. G. Charge Disproportionation in Tetragonal La_2MoO_5, a Small Band Gap Semiconductor Influenced by Direct Mo-Mo Bonding. *J. Am. Chem. Soc.,* **2015,** 137, 1245-1257.

(10) Cortese, A. J.; Abeysinghe, D.; Wilkins, B.; Smith, M. D.; Morrison, G.; zur Loye, H. C. High-Temperature Salt Flux Crystal Growth of New Lanthanide Molybdenum Oxides, $Ln_5Mo_2O_{12}$ Ln = Eu, Tb, Dy, Ho, and Er:

Magnetic Coupling within Mixed Valent Mo(IV/V) Rutile-Like Chains. *Inorg, Chem.,* **2015,** 54, 11875-11882.

(11) Chi, L. S.; Britten, J. F.; Greedan, J. E. Synthesis, Structure And Magnetic Properties Of The S=1/2, One-Dimensional Antiferromagnet, $Y_5Re_2O_{12}$. *J. Solid State Chem.,* **2003,** 172, 451-457.

(12) Miura, Y.; Yasui, Y.; Sato, M.; Igawa, N.; Kakurai, K. New-Type Phase Transition Of Li_2RuO_3 With Honeycomb Structure. *J. Phys. Soc. Jpn.,* **2007,** 76, 033705.

(13) Westman, S. Note On A Phase Transition In VO_2. *Acta Chem. Scand.,* **1961,** 15, 217-217.

(14) Kawada, I.; Kimizuka, N.; Nakahira, M. Crystallographic Investigations Of Phase Transition Of VO_2. *J. Appl. Crystallogr.,* **1971,** 4, 343-347.

(15) Hiroi, Z. Structural Instability Of The Rutile Compounds And Its Relevance To The Metal-Insulator Transition Of VO_2. *Prog. Solid State Chem.,* **2015,** 43, 47-69.

(16) Wentzcovitch, R. M.; Schulz, W. W.; Allen, P. B. VO_2 - Peierls Or Mott-Hubbard - A View From Band Theory. *Phys. Rev. Lett.,* **1994,** 72, 3389-3392.

(17) Cavalleri, A.; Toth, C.; Siders, C. W.; Squier, J. A.; Raksi, F.; Forget, P.; Kieffer, J. C. Femtosecond Structural Dynamics In VO_2 During An Ultrafast Solid-Solid Phase Transition. *Phys. Rev. Lett.,* **2001,** 87, 4.

(18) Newsome, L.; Cleary, A.; Morris, K.; Lloyd, J. R. Long-Term Immobilization of Technetium via Bioremediation with Slow-Release Substrates. *Environ. Sci. Technol.,* **2017,** 51, 1595-1604.

(19) Jaisi, D. P.; Dong, H. L.; Plymale, A. E.; Fredrickson, J. K.; Zachara, J. M.; Heald, S.; Liu, C. X. Reduction And Long-Term Immobilization Of Technetium By Fe(II) Associated With Clay Mineral Nontronite. *Chem. Geol.,* **2009,** 264, 127-138.

(20) Wallwork, K. S.; Kennedy, B. J.; Wang, D. The high resolution powder diffraction beamline for the Australian Synchrotron. *AIP Conference Proceedings,* **2007,** 879, 879-882.

(21) Liss, K. D.; Hunter, B.; Hagen, M.; Noakes, T.; Kennedy, S. Echidna - the new high-resolution powder diffractometer being built at OPAL. *Physica B.,* **2006,** 385-86, 1010-1012.

(22)   Larson, A. C.; Von Dreele, R. B. *General Structure Analysis System. LANSCE, MS-H805, Los Alamos, New Mexico*, 1994.

(23)   Glover, C.; McKinlay, J.; Clift, M.; Barg, B.; Boldeman, J.; Ridgway, M.; Foran, G.; Garrett, R.; Lay, P.; Broadbent, A. Status of the x-ray absorption spectroscopy (XAS) beamline at the Australian synchrotron. *AIP Conf. Proc.,* **2007,** 882, 884-886.

(24)   Blanchard, P. E. R.; Reynolds, E.; Kennedy, B. J.; Ling, C. D.; Zhang, Z. M.; Thorogood, G.; Cowie, B. C. C.; Thomsen, L. An unconventional method for measuring the Tc L-3-edge of technetium compounds. *J. Sync. Rad.,* **2014,** 21, 1275-1281.

(25)   Ravel, B.; Newville, M. ATHENA, ARTEMIS, HEPHAESTUS: data analysis for X-ray absorption spectroscopy using IFEFFIT. *J. Sync. Rad.,* **2005,** 12, 537-541.

(26)   Rogers, D. B.; Shannon, R. D.; Sleight, A. W.; Gillson, J. L. Crystal Chemistry Of Metal Dioxides With Rutile-Related Structures. *Inorg. Chem.,* **1969,** 8, 841-849.

(27)   Bolzan, A. A.; Fong, C.; Kennedy, B. J.; Howard, C. J. Structural Studies Of Rutile-Type Metal Dioxides. *Acta Crystallogr., Sect. B: Struct. Sci* **1997,** 53, 373-380.

(28)   Rao, K. V. K.; Naidu, S. V. N.; Iyengar, L. Thermal Expansion Of Rutile And Anatase. *J. Am. Ceram. Soc.,* **1970,** 53, 124.

(29)   Dose, W. M.; Donne, S. W. Thermal Expansion Of Manganese Dioxide Using High-Temperature In Situ X-Ray Diffraction. *J. Appl. Crystallogr.,* **2013,** 46, 1283-1288.

(30)   Mary, T. A.; Evans, J. S. O.; Vogt, T.; Sleight, A. W. Negative thermal expansion from 0.3 to 1050 Kelvin in ZrW_2O_8. *Science,* **1996,** 272, 90-92.

(31)   Goodwin, A. L.; Kepert, C. J. Negative thermal expansion and low-frequency modes in cyanide-bridged framework materials. *Phys. Rev. B,* **2005,** 71, 140301.

(32)   Goodenough, J. B. 2 Components Of Crystallographic Transition In VO_2. *J. Solid State Chem.,* **1971,** 3, 490-500.

(33)   Bolzan, A. A.; Fong, C.; Kennedy, B. J.; Howard, C. J. A Powder Neutron-Diffraction Study Of Semiconducting And Metallic Niobium Dioxide. *J. Solid State Chem.,* **1994,** 113, 9-14.

(34)   Burdett, J. K. Electronic Control Of The Geometry Of Rutile And Related Structures. *Inorg. Chem.,* **1985,** 24, 2244-2253.

(35)   Scanlon, D. O.; Watson, G. W.; Payne, D. J.; Atkinson, G. R.; Egdell, R. G.; Law, D. S. L. Theoretical and Experimental Study of the Electronic Structures of MoO_3 and MoO_2. *J. Phys. Chem. C,* **2010,** 114, 4636-4645.
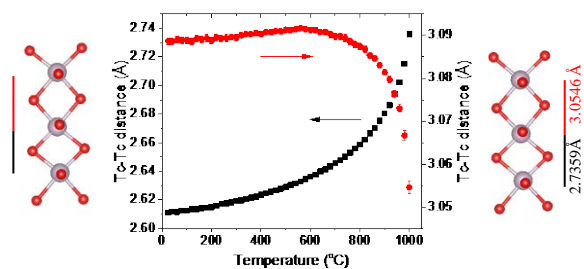
TcO$_2$ has a monoclinic structure in space group $P2_1/c$ between 25 and 1000 °C as established using a combination of synchrotron X-ray and neutron powder diffraction methods and is found to remain monoclinic in the same space group. The thermal expansion of the lattice is highly anisotropic with negative thermal expansion of the b-axis observed above 700 °C. This appears to be a consequence of weakening of the Tc-Tc bonds that form along the a-axis.